Lattice dynamics of incipient ferroelectric rutile TiO_2

F. Gervais
*Max-Planck-Institut für Festkörperforschung, Heisenbergstrasse 1, D-7000 Stuttgart 80, Federal Republic of Germany and Centre de Recherches sur la Physique des Hautes Températures, Centre National de la Recherche Scientifique, F-45045 Orléans, France**

W. Kress
Max-Planck-Institute für Festkörperforschung, Heisenbergstrasse 1, D-7000 Stuttgart 80, Federal Republic of Germany
(Received 6 May 1983)

Phonon dispersion curves in rutile TiO_2 have been calculated with a rigid-ion model and a shell model. The shell model closely reproduces experimental data. The hardening of soft ferroelectric Γ_1^- and Γ_5^+ TO modes with increasing temperature, which is observed experimentally, is found to be due to a small simultaneous decrease in effective ionic charge and oxygen polarizability. The decrease in both quantities can be understood in terms of fourth-order inter-ion and oxygen core-shell anharmonic interactions.

I. INTRODUCTION

The importance of the polarizability of the oxygen ion for ferroelectricity and related phenomena in crystals has been emphasized by Migoni, Bilz, and Bäuerle.[1] The phenomenon has been mainly studied in perovskite crystals.[2–7] One of the purposes of this paper is to discuss to what extent similar ideas might be relevant to crystals with the rutile structure D_{4h}^{14} ($P4_2/mnm$). Rutile TiO_2 itself exhibits incipient ferroelectric properties while fluorides with D_{4h}^{14} symmetry behave "normally". The same situation is found in perovskites.[1] More interesting is to note that different oxides with the rutile structure exhibit pronounced differences in their physical properties. TiO_2 is, e.g., an incipient ferroelectric with soft modes associated with a dielectric constant which reaches 250 at low temperature.[8] SnO_2 and GeO_2 do not show any soft modes like TiO_2 even though the ionic radii of Sn^{4+} or Ge^{4+} differ from that of Ti^{4+} by only 10% (Ref. 9) and even the molecular polarizabilities of TiO_2 and SnO_2 are very similar. Nevertheless, the theory developed for perovskites[1] and SbSI (Ref. 6) is still applicable. The point is the following: The strong polarizability of oxygen in the presence of a transition-metal ion is anisotropically enhanced due to hybridization between oxygen p states and transition-metal d states.[1] This mechanism could thus explain the incipient ferroelectric character of TiO_2 whereas the oxides of tin or germanium, which do not belong to the class of transition-metal elements, do not exhibit the same behavior. Other oxides with transition-metal elements have very interesting properties: NbO_2 and VO_2 undergo a structural phase transition to the D_{4h}^{14} structure at $\sim$1080 and 340 K, respectively, where they become metallic (see a review of their properties in Ref. 10, for example). Their structures are more complicated below the transition temperature but the main structural distortion consists in pairing of one-half of the metallic ions along the direction of the c axis of the rutile structure. Whether the phase transition is triggered by lattice instabilities or electronic entropy is still open to discussion.[11,12]

The thermophysical properties of solids are caused or are strongly influenced by the lattice dynamics. The measurement of phonon dispersion curves of rutile TiO_2 by Traylor *et al.*,[13] opened the way to computer calculations of the lattice-dynamical properties. Traylor *et al.*[13] described the dispersion curves of TiO_2 within the framework of a shell model with many adjustable parameters. The results were very unsatisfactory. Previous calculations were based on zone-center frequencies only. Results were discussed by Traylor *et al.*[13] They showed that the parameters of Katiyar and Krishnan[14] lead to imaginary frequencies for some modes near the Brillouin-zone boundary. One further important comment within the context of this paper is that the calculation in Ref. 14 gives a soft TO Γ_1^- mode frequency which is a factor of 2.3 higher than the measured frequency. This model, therefore, does not appear to constitute a good basis for the understanding of ferroelectriclike properties. The main conclusions of the calculations of Traylor *et al.*[13] were the following: (i) Only tensorial force field for all interactions (except the second-neighbor oxygen-oxygen interactions) is able to give acceptable qualitative agreement with the data, (ii) a shell model improves the agreement compared with a rigid-ion model, and (iii) some modes could not be well described with this model. Since oxides with the rutile structure are of particular physical interest, it seems to be worthwhile to reinvestigate their lattice vibrations while the purpose of this work is to construct a model as simple as possible to elucidate the physics of lattice vibrations and their relation to instabilities.

II. RIGID-ION MODEL

For the sake of simplicity, we first attempt to describe the phonon dispersion curves of TiO_2 with a rigid-ion (RI) model. The dynamical matrix is written

$$\underline{D}^{\mathrm{RI}}(\vec{q})=\underline{R}(\vec{q})+\underline{Z}\,\underline{C}(\vec{q})\underline{Z}\ , \tag{1}$$

 ©1983 The American Physical Society

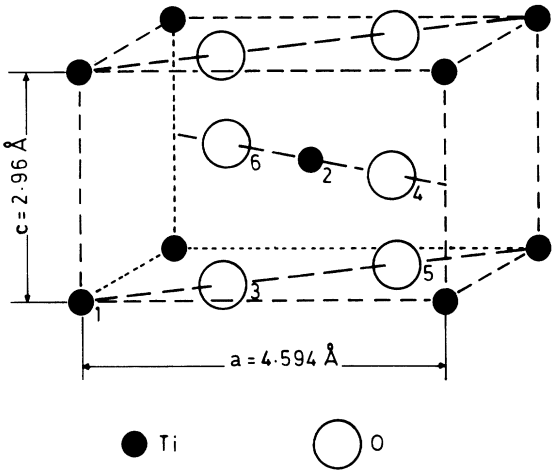

FIG. 1. Rutile structure.

where $\underline{Z}$ is an effective ionic charge tensor, $\underline{C}$ the matrix of the Coulomb coefficients, and $\underline{R}$ the short-range repulsive force-constant matrix. We start with the most general form of the dynamical matrix compatible with symmetry. There are two titanium atoms in the primitive unit cell (Fig. 1), which occupy positions (0,0,0) and $(\frac{1}{2},\frac{1}{2},\frac{1}{2})$. Oxygen atoms form octahedra around each Ti ion (Fig. 2). The octahedron centered at position $(\frac{1}{2},\frac{1}{2},\frac{1}{2})$ is rotated by $\pi/2$ about the c axis with respect to the octahedron centered at position (0,0,0). There are two different Ti-O distances within the octahedron. Two oxygen atoms are linked to a Ti atom within a (001) plane (Ti_1-O_3, Ti_2-O_4, or Ti_2-O_6) (for notation see Figs. 1 and 2). The four other Ti-O distances are equal to 1.944 Å. The dynamical matrix is 18×18. By symmetry, the structure of 3×3 submatrices for all nearest-neighbor (atom κ)—(atom κ') interactions is of the form

$$\begin{bmatrix} \alpha_{\kappa\kappa'} & \gamma_{\kappa\kappa'} & \delta_{\kappa\kappa'} \\ \gamma_{\kappa\kappa'} & \alpha_{\kappa\kappa'} & \delta_{\kappa\kappa'} \\ \mu_{\kappa\kappa'} & \mu_{\kappa\kappa'} & \beta_{\kappa\kappa'} \end{bmatrix} .$$

For all interactions of pairs of atoms lying in a (001) plane, the matrix is further simplified to the general form

$$\begin{bmatrix} \alpha & \gamma & 0 \\ \gamma & \alpha & 0 \\ 0 & 0 & \beta \end{bmatrix} .$$

For the sake of clarity in notation, the short-range—force-constant matrix is explicitly given in Table I for zero wave vector. According to Ref. 13, the O_3-O_4—type interaction between second-nearest neighbors (bond length 2.78 Å) is

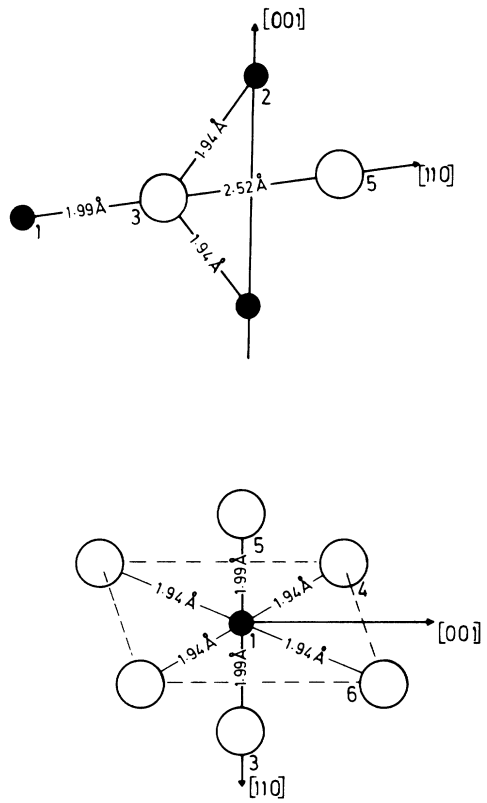

FIG. 2. Nearest neighbors of titanium and oxygen in the rutile structure (Ref. 16).

TABLE I. Notations used for the dynamical matrix for zero wave vectors.

$$\underline{\phi} = \begin{array}{c} \\ \text{Ti} \\ \\ \\ \text{O} \\ \\ \end{array} \begin{array}{c} \overbrace{1 \quad 2}^{\text{Ti}} \quad \overbrace{3 \quad 4 \quad 5 \quad 6}^{\text{O}} \\ \begin{bmatrix} \underline{\phi}_{11} & \underline{\phi}_{12} & \underline{\phi}_{13} & \underline{\phi}_{14} & \underline{\phi}_{15} & \underline{\phi}_{16} \\ \underline{\phi}_{21} & \underline{\phi}_{22} & \underline{\phi}_{23} & \underline{\phi}_{24} & \underline{\phi}_{25} & \underline{\phi}_{26} \\ \underline{\phi}_{31} & \underline{\phi}_{32} & \underline{\phi}_{33} & \underline{\phi}_{34} & \underline{\phi}_{35} & \underline{\phi}_{36} \\ \underline{\phi}_{41} & \underline{\phi}_{42} & \underline{\phi}_{43} & \underline{\phi}_{44} & \underline{\phi}_{45} & \underline{\phi}_{46} \\ \underline{\phi}_{51} & \underline{\phi}_{52} & \underline{\phi}_{53} & \underline{\phi}_{54} & \underline{\phi}_{55} & \underline{\phi}_{56} \\ \underline{\phi}_{61} & \underline{\phi}_{62} & \underline{\phi}_{63} & \underline{\phi}_{64} & \underline{\phi}_{65} & \underline{\phi}_{66} \end{bmatrix} \end{array} ,$$

where, with the definition of the 3×3 matrix

$$\varphi_{ij}^{a,b,c} = \begin{bmatrix} a\alpha_{ij} & c\gamma_{ij} & 0 \\ c\gamma_{ij} & a\alpha_{ij} & 0 \\ 0 & 0 & b\beta_{ij} \end{bmatrix} ,$$

we have

$$\begin{aligned}
&\underline{\phi}_{11} = \varphi_{\bar{1}\bar{1}}^{2,-2,2} \\
&\underline{\phi}_{12} = \underline{\phi}_{21} = \varphi_{\bar{1}2}^{8,-8,0} , \\
&\underline{\phi}_{13} = \underline{\phi}_{31} = \underline{\phi}_{15} = \underline{\phi}_{51} = \varphi_{\bar{1}3}^{1,-1,-1} , \\
&\underline{\phi}_{14} = \underline{\phi}_{41} = \underline{\phi}_{16} = \underline{\phi}_{61} = \varphi_{\bar{1}4}^{2,-2,2} , \\
&\underline{\phi}_{22} = \varphi_{\bar{1}\bar{1}}^{2,-2,-2} , \\
&\underline{\phi}_{23} = \underline{\phi}_{32} = \underline{\phi}_{25} = \underline{\phi}_{52} = \varphi_{\bar{1}4}^{2,-2,-2} , \\
&\underline{\phi}_{24} = \underline{\phi}_{42} = \underline{\phi}_{26} = \underline{\phi}_{62} = \varphi_{\bar{1}3}^{1,-1,1} , \\
&\underline{\phi}_{33} = \underline{\phi}_{55} = \varphi_{\bar{3}\bar{3}}^{2,-2,-2} , \\
&|\underline{\phi}_{34}| = |\underline{\phi}_{43}| = |\underline{\phi}_{36}| = |\underline{\phi}_{63}| = |\underline{\phi}_{45}| = |\underline{\phi}_{54}| = |\underline{\phi}_{56}| = |\underline{\phi}_{65}| , \\
&\underline{\phi}_{35} = \underline{\phi}_{53} = \varphi_{\bar{3}5}^{1,-1,-1} , \\
&\underline{\phi}_{44} = \underline{\phi}_{66} = \varphi_{\bar{3}\bar{3}}^{2,-2,2} , \\
&\underline{\phi}_{46} = \underline{\phi}_{64} = \varphi_{\bar{3}5}^{1,-1,1} .
\end{aligned}$$

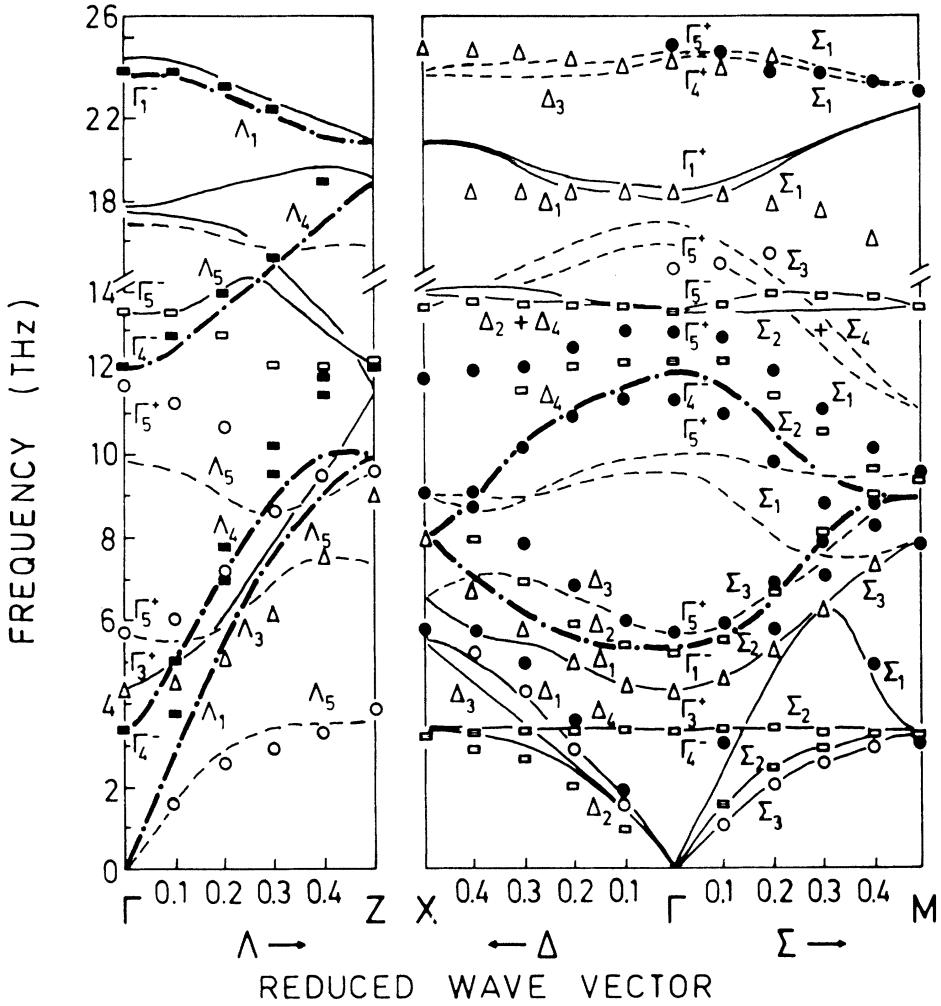

FIG. 3. Comparison of phonon dispersion calculated with the rigid-ion model (full curves) with that measured by Traylor *et al.* (symbols, Ref. 13).

assumed to be so weak that only the radial components have to be taken into account. Ti_1-Ti_1 interactions are only taken into account for those pairs which have the shortest bond length (2.96 Å). The Ti_1-Ti_2 interactions, which have a bond length of 3.57 Å, are not neglected *a priori*, and are included in the dynamical matrix. These Ti_1-Ti_2 interactions were not considered by Traylor *et al.*[13] The structural arrangement of nearest neighbors of titanium and oxygen is displayed in Fig. 2. The translational invariance condition for both short-range forces and Coulomb matrices determines the self-interaction. The rotational-invariance condition, which apparently was not considered in Ref. 13, gives two further relations between the parameters. It is convenient to choose γ_{35} and δ_{14} as nonadjustable parameters. In addition we find that μ_{14} does not differ much from δ_{14} and impose therefore the additional condition $\delta_{14}=\mu_{14}$. This condition has little effect on the results.

In a preliminary stage, we neglect the O_i-O_i ($i=3$–6) short-range interactions (bond lengths 2.96 Å) as well as all Ti-Ti interactions. One of the purposes of our work is to find out which parameters have the main influence on the softening of the Γ_1^- and on the lowest-frequency Γ_5^+ TO ferroelectric soft modes. The parameters were adjusted step-by-step one after the other. This process obviously is time consuming but it elucidates the influence of the different parameters on the phonon dispersion curves. In the first stage of the calculations, we tried to reproduce all frequencies at the zone center simultaneously with the lowest-frequency phonons at the points Z and M. Note that the determination of all TO and LO frequencies at the Γ point of this noncubic structure, requires the diagonalization of two dynamical matrices with different Coulomb parts for phonons propagating parallel and perpendicular to the c axis. Once satisfactory agreement was achieved, we worked with complete dispersion curves. At that stage, only minor refinements of the parameters were necessary to improve the fit. The results are shown in Fig. 3. They appear surprisingly good in view of the fact that the rigid-ion model does not take into account polarizability effects which are expected to play an important role. Almost all phonon dispersion branches are well reproduced with the rigid-ion model, except (i) the nonsoft Γ_5^+ TO modes and the branches to which they belong. One of these modes is 14% too high and the other is 14% too low. The TO-LO splittings associated with them and, therefore, the infrared oscillator strengths, are about 40% too small. On the other hand, the extremely large oscilla-

TABLE II. Best-fit parameters of analysis of experimental dispersion curves. RIM indicates a rigid-ion model and SM indicates a shell model. Units of force-constant parameters are 10^5 dyn/cm.

		RIM	SM
	Z/Z_0	0.67	0.83
Ti-O	α_{13}	0.69	1.33
In (001) plane	β_{13}	−0.17	−0.40
	γ_{13}	1.26	2.10
Out of plane	α_{14}	0.27	0.30
	β_{14}	0.99	1.58
	γ_{14}	0.87	0.85
O-O	α_{35}	0.6	0.505
In plane	β_{35}	0.63	0.58
	Weak interaction parameters		
Out of plane	ϕ_{34}	0.1	0.04
Ti-Ti	α_{12}	0.07	0.06
	β_{12}		0.035
	γ_{12}		0.035
	α_{11}		0.105
	SM parameters		
			$Y=2.75e$
			$k_{\parallel}=14$
			$k_{\perp}=16$

tor strengths of both ferroelectriclike Γ_1^- and Γ_5^+ TO modes and the large TO-LO splittings they yield are quite well described by the model. (ii) The frequency of the acoustic branch Λ_1 at Z_1 is about 18% too low. (iii) Although the highest frequency Γ_1^+ mode agrees well with the experimental frequency, the corresponding Δ_1 and Σ_1 branches are poorly reproduced.

The parameters used in the calculation of the phonon dispersion curves which are shown in Fig. 3 are given in Table II. The seven main parameters are:

(i) The effective charge. A change of 1% of this parameter does not only shift the ferroelectriclike TO modes by 10% but also shifts the branches associated with the low-frequency Γ_4^- and Γ_3^+ phonons to at least the same extent (10%). Since TO-LO splittings of ferroelectric modes are well reproduced with this model, the effective charge obviously agrees perfectly with the straightforward determination reported in Ref. 15.

(ii) The α_{13}, γ_{13} and α_{14}, γ_{14} parameters, which mainly influence all vibrations with eigenvectors in the (001) planes, including the Γ_5^+ soft mode. The structure becomes unstable (imaginary frequencies) if one decreases α_{13}, γ_{13}, α_{14}, or γ_{14} by 20–30%.

(iii) The β_{13} and β_{14} force constants which control the frequencies of the phonons whose eigenvectors are parallel to the c axis, including the Γ_1^- soft mode. A decrease of 15% of β_{14} is sufficient to destabilize the structure.

Parameters which describe the oxygen-oxygen short-range interactions are less "critical". The α_{35} force constant only influences the two high-frequency branches associated with the Γ_1^+ and Γ_4^+ phonons and that to a small extent. The β_{35} force constant influences only slightly the branch associated with the Γ_5^- phonon. The radial force-constant parameter for the 3—4 type interactions is found to be small. Therefore, the nonradial interactions, which will be still smaller, can be neglected. Finally, the introduction of a weak Ti_1-Ti_2 interaction parameter improves the fit for phonon branches associated with Γ_5^+ modes, especially at the zone-boundary points.

If we compare our parameters with those reported by Traylor *et al.*,[13] we find that the two sets of parameters are similar. Note that some signs are reversed due to different definitions of the parameters. The calculations of Traylor *et al.* reproduced low-frequency phonon dispersion curves as well as ours, except that the soft-mode branch in the Λ direction is much too low in Ref. 13. In the medium-frequency range, Traylor *et al.* encountered problems similar to ours concerning the Γ_5^+ modes. The high-frequency Λ_4 branch is described correctly in our calculation, whereas significant disagreement is found in Ref. 13. The main discrepancies with experimental data concern the LO-phonon branches. Traylor *et al.* obtain frequencies which are too low to fit the oscillator strengths of soft TO modes. As a result, they reported an effective ionic charge which is about 18% smaller than the value deduced from experimental TO-LO splittings. Our value fits the experiments correctly.[15]

III. SHELL MODEL

From the observation of refractive indices for many crystals in the visible region[17] it is possible to estimate the electronic polarizabilities. The calculations are based on the assumptions of the additivity of electronic polarizabilities of individual ions and of a Lorentz field with cubic symmetry. The application of the Lorentz expression,

$$\frac{4\pi}{3V}(2\alpha_{\mathrm{Ti}}+4\alpha_{\mathrm{O}})=\frac{\epsilon_\infty-1}{\epsilon_\infty+2}\ , \tag{2}$$

yields the oxygen polarizabilities $\alpha_{\mathrm{O}}^{\parallel}=2.5$ Å^3 parallel to the c axis and $\alpha_{\mathrm{O}}^{\perp}=2$ Å^3. V is the volume of the unit cell and ϵ_∞ is the high-frequency dielectric constant. The approximate value $\alpha_{\mathrm{Ti}}=0.2$ Å^3 has been used in this calculation.[17]

The shell model implies that the ion is considered as a positively-charged inner core and an outer electron shell which carries the charge Ye. The shell is coupled to its own core by a force constant k. The electronic polarizability of the ion is given by

$$\alpha=\frac{(Ye)^2}{k+2f}\ , \tag{3}$$

wherer f represents the short-range coupling constant with adjacent ions. We have neglected the polarizability of Ti in our calculation since $\alpha_{\mathrm{Ti}}/\alpha_{\mathrm{O}}$ is estimated to be 10%.

Within the shell model, the dynamical matrix is written (see, for example, Ref. 18 or 19)

$$\underline{D}=\underline{R}-(\underline{T}+\underline{Z}\,\underline{C}\,\underline{Y})(\underline{S}+\underline{K}+\underline{Y}\,\underline{C}\,\underline{Y})^{-1}(\underline{T}^{\dagger}+\underline{Y}\,\underline{C}\,\underline{Z})\ . \tag{4}$$

The matrices $\underline{T}$ and $\underline{S}$ correspond to the short-range

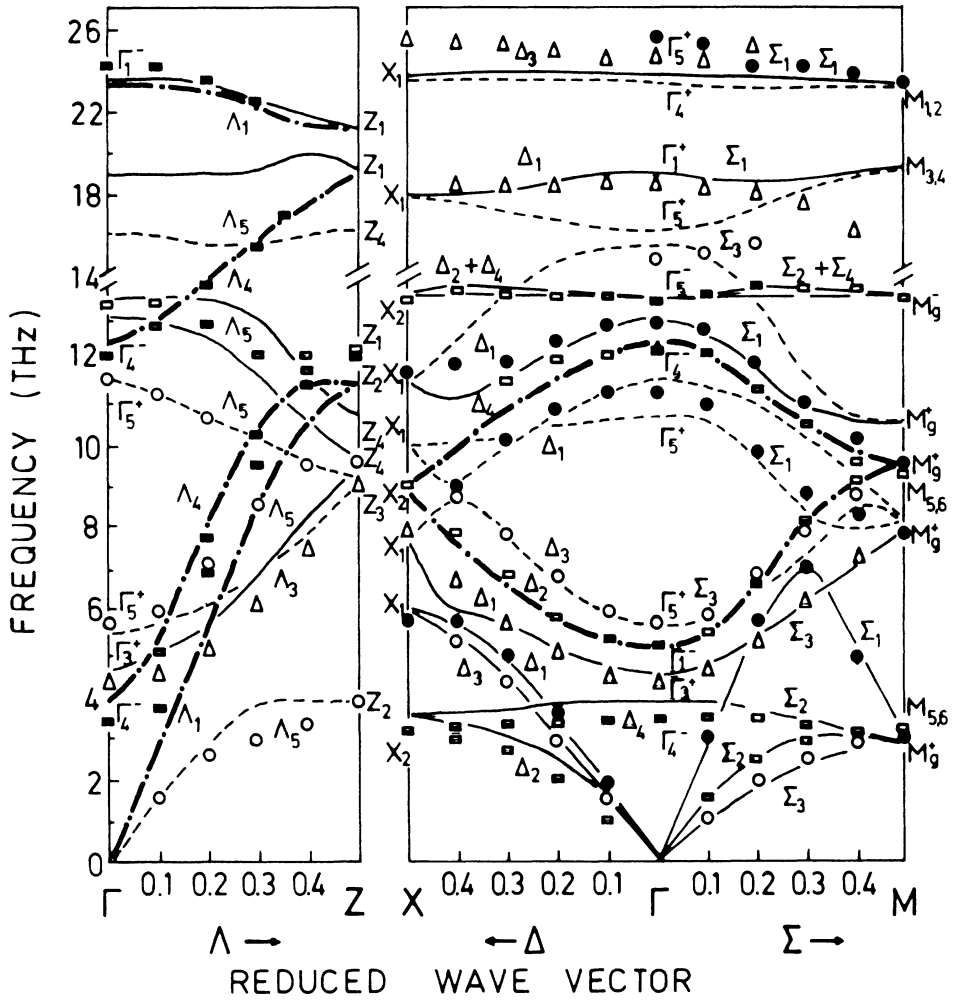

FIG. 4. Phonon dispersion calculated with the shell model and parameters given in Table II, compared with experimental data (Ref. 13).

electron-ion and electron-electron coupling, respectively. $\underline{K}$ denotes the diagonal matrix which is made out of the core-shell coupling constants k_κ. For the nonpolarizable ions (Ti) $k_{\mathrm{Ti}}=\infty$. If we take into account only shell-shell interionic interactions we obtain $\underline{R}=\underline{T}=\underline{S}$.

The best results of our shell model are shown in Fig. 4. We first note an important improvement with respect to the calculations with the rigid-ion model. The calculated curves agree everywhere with experimental data within a few percent. Again, results are much more satisfactory than those reported in Ref. 13. Compared to the rigid-ion-model calculations, most of the seven main parameters have now larger values. The Ti-O short-range force constants α_{13}, γ_{13}, or β_{14} are increased by 93%, 67%, and 60%, respectively. The effective ionic charge is increased by 24%. This "hardening" of the lattice is compensated by the polarizability of the oxygen ions which tends to soften the crystal lattice. The new set of parameters is thus physically realistic and consistent with the rigid-ion-model parameters. We did not succeed in reproducing the polarizability deduced from ϵ_∞ within this—probably too simple—description. Core-shell force constants $k_{\|}=14\times10^5$ dyn/cm, $k_\perp=16\times10^5$ dyn/cm, and $Y=2.75$ (see Table II) yield $\alpha_0^{\|}=1.1$ Å^3 and $\alpha_0^{\perp}=0.97$ Å^3. Those values represent half of the value which has been determined from experiment. Increasing the charge Y or decreasing the k destabilizes the lattice in such a way that it is no longer possible to compensate this effect by increasing the short-range force constants. Note that the effective charge has now a value of $Z/Z_0=0.83$ where Z_0 is the chemical valence. The consideration of an anisotropic core-shell coupling is not necessary to get the best fit to phonon dispersion curves. Thus, anisotropy was introduced only to be consistent with the slight anisotropy of the high-frequency dielectric constant. If the oxygen polarizability is chosen to be as high as possible, Ti-Ti interactions (see Table II) are necessary to stabilize the lattice. The Ti-Ti interaction parameters remain, however, small compared to the shortest-range force constants. The experimental data[13] show the existence of four low-frequency optical-phonon branches which are coupled to the acoustic phonons. Two of the four branches are found to soften with decreasing temperature. This indicates the unstable character of this structure. This intrinsic instability makes calculated results very sensitive to slight variations of the parameters, especially in the shell model in which the balance between forces is even more delicate than in the rigid-ion model.

TABLE III. Relative frequency shifts induced by change of parameters describing the oxygen polarizability and the effective ionic charge.

	Γ_5^+ (189 cm^{-1})	Γ_1^- (172 cm^{-1})	Γ_3^+ (143 cm^{-1})	Γ_4^- (113 cm^{-1})
$\Delta Z/Z=-1\%$	4%	16%	−10%	17%
$\Delta Y/Y=-1\%$	5%	3%	2%	5%
$\Delta k_{\parallel}/k_{\parallel}=8\%$		5%		9%
$\Delta k_{\perp}/k_{\perp}=8\%$	10%		5%	

IV. DISCUSSION

Having derived a simple model which is able to reproduce phonon dispersion curves satisfactorily, we return to the discussion of incipient ferroelectric properties of rutile. The aim is to find which parameters can reproduce the softening of the Γ_1^- and Γ_5^+ modes and leaves the other frequencies essentially constant. If we neglect the thermal expansion of the lattice, the six atoms stay in their positions and no significant change of short-range force-constant parameters is therefore expected when the temperature is decreased. On the other hand, we know from experiment that ϵ_∞ increases slightly with decreasing temperature (see discussion and bibliography in Ref. 8). A rough estimate based on the extrapolation of room-temperature data and Eq. (2) indicates, however, that the increase of α_0 does not exceed 2% per 1000 K. On the other hand, we know the temperature dependence of polar-optical phonons.[20] The effective ionic charge, deduced from TO-LO splittings, is thus found[15] to decrease by 2% on heating from 300 K up to 1400 K. This result confirms earlier conclusions of Samara and Peercy[8] concerning the decrease of Z with increasing temperature, which was based on dielectric-constant data. The main relative frequency shifts, which are induced by small changes of effective charge and by the change of parameters (Y or k), have been calculated with our shell model and results are given in Table III. A decrease of oxygen polarizability (via decrease of Y or increase of k) and (or) of the effective charge clearly hardens the ferroelectric Γ_1^- and the lowest TO Γ_5^+ modes. Those upward shifts are accompanied by shifts of neighboring Γ_3^+ and Γ_4^- modes. Experimentally, the Γ_3^+ frequency does not shift significantly with increasing temperature. Table III shows, however, that a decrease of polarizability raises the frequency whereas a decrease of Z lowers it. The two effects can therefore counterbalance each other so that the Γ_3^+ frequency remains nearly constant. On the other hand, the model predicts a simultaneous concomitant upward shift of Γ_4^- frequency with the hardening of Γ_1^- mode. Unfortunately, the temperature dependence of the Γ_4^- mode which is infrared and Raman inactive, is unknown. It is, however, instructive to compare data at TiO_2 with other nonferroelectric crystals where they are available, MgF_2 for example.[21] Except for the soft modes in TiO_2, the phonon dispersion curves of the two materials are similar. As in TiO_2, the Γ_3^+ mode in MgF_2 is found at low frequency. On the other hand, at room temperature, the Γ_4^- mode frequency in MgF_2 is twice as high as in TiO_2, in spite of the general tendency of phonon energies to be lower in MgF_2 than in TiO_2. It is therefore not unrealistic to expect a hardening of this mode on heating TiO_2.

In conclusion, the soft-mode behavior of TO phonons polarized parallel (Γ_1^-) and perpendicular (Γ_5^+) to the c axis of TiO_2 can be accounted by a small simultaneous change of only two parameters: the effective ionic charge and the oxygen polarizability. The decrease of oxygen polarizability is ascribed to the increase with temperature of the fourth-order anharmonic core-shell force constant of oxygen.[2] The physical reason for the decrease of the effective ionic charge on heating is not straightforward. Following Samara and Peercy,[8] we believe that the phenomenon might be related to redistributions of charges and overlap when the ions are displaced by the lattice vibrations. The charge redistribution is not taken into account in our simple shell model. (This might be the reason why the model accounts only partially for the measured oxygen polarizability.) The increase of thermal amplitude of vibration with increasing temperature can be expected to result in additional overlap and, therefore, a slight decrease of the effective ionic charge. In fact, lattice thermal expansion cancels a part of the increase of vibrational amplitude, but the balance could be in favor of additional overlap since the conjugated effects of fourth-order intra-oxygen and interionic anharmonicities do stabilize the motions of titanium against the oxygen octahedron.

ACKNOWLEDGMENT

Valuable discussions with H. Bilz are gratefully acknowledged.

*Present address.

[1]R. Migoni, H. Bilz, and D. Bäuerle, Phys. Rev. Lett. 37, 1155 (1976).

[2]H. Bilz, A. Bussmann, G. Benedek, H. Büttner, and D. Strauch, Ferroelectrics 25, 339 (1980).

[3]A. Bussmann, H. Bilz, R. Roenspiess, and K. Schwarz, Ferroelectrics 25, 343 (1980).

[4]A. Bussmann-Holder, H. Bilz, D. Bäuerle, and D. Wagner, Z. Phys. B 41, 353 (1981).

[5]J. L. Servoin, Y. Luspin, and F. Gervais, Phys. Rev. B 22, 5501 (1980).

[6]M. Massot, M. K. Teng, J. F. Vittori, M. Balkanski, S. Ziol-

kiewicz, F. Gervais, and J. L. Servoin, Ferroelectrics 45, 237 (1982); M. Balkanski, M. K. Teng, M. Massot, and H. Bilz, Ferroelectrics 26, 737 (1980).
[7]D. Rytz, J. L. Servoin, and F. Gervais, Ferroelectrics 38, 817 (1981).
[8]G. A. Samara and P. S. Peercy, Phys. Rev. B 7, 1131 (1973).
[9]R. D. Shannon, Acta Crystallogr. A32, 751 (1976).
[10]J. B. Goodenough, *Progress in Solid State Chemistry,* edited by H. Reiss (Pergamon, Oxford, 1971), Vol. 5, p. 145.
[11]D. Paquet and P. Leroux-Hugon, Phys. Rev. B 22, 5284 (1980).
[12]F. Gervais, Phys. Rev. B 23, 6580 (1981).
[13]J. G. Traylor, H. G. Smith, R. M. Nicklow, and M. K. Wilkinson, Phys. Rev. B 3, 3467 (1971).
[14]R. S. Katiyar and R. S. Krishnan, Phys. Lett. 25A, 525 (1967).
[15]F. Gervais, Solid State Commun. 18, (1976).
[16]W. H. Baur, Acta Crystallogr. 9, 515 (1956).
[17]J. R. Tessman, A. H. Kahn, and W. Shockley, Phys. Rev. 92, 890 (1953).
[18]G. Venkataraman, L. A. Feldkamp, and V. C. Sahni, *Dynamics of Perfect Crystals,* (MIT Press, Cambridge, 1975).
[19]H. Bilz and W. Kress, *Phonon Dispersion Relations in Insulators* (Springer, Berlin, 1979).
[20]F. Gervais and B. Piriou, Phys. Rev. B 10, 1642 (1974).
[21]R. Almairac, J. L. Sauvajol, C. Benoit, and A. M. Bon, J. Phys. C 11, 3157 (1978).